Anatomic Study on Neuroendoportal Transcortical Approach to Lateral Ventricles

Filippo Gagliardi[1], Martina Piloni[1], Michele Bailo[1], Cristian Gragnaniello[2], Nicola Boari[1], Carmine A. Donofrio[1], Lina R. Barzaghi[1], Jody F. Capitanio[1], Anthony J. Caputy[2], Pietro Mortini[1]

BACKGROUND: **Resection of intraventricular lesions remains a challenge for modern neurosurgery. Endoscopy has provided great advantages in ventricular surgery, even if limited in terms of operability, due to the restricted working channel and impossibility for bimanual surgical manipulation. Tubular approaches have been considered as an option, enabling the use of microsurgical techniques, minimizing violation of brain tissue. The aim of our study was to describe and critically evaluate the use of portal surgery to access lateral ventricles in terms of surgical exposure and operability.**

METHODS: **A microanatomic laboratory cadaver study was conducted with a stepwise description of the surgical technique. The operability score was applied for quantitative analysis of surgical operability, and an illustrative case is reported.**

RESULTS: **Through the anterior approach, the neuroport provides maximal operability at the foramen of Monro and the posterior aspect of the frontal horn, while through the posterior approach maximal operability is achieved in the paratrigonal area. Endoscopic assistance does not affect operability but provides adjunctive exposure in blind spots, as the roof of the frontal horn, the most anterior aspect of the temporal and occipital horn.**

CONCLUSIONS: **Ventricular tubular systems provide adequate visualization, with minimal brain retraction, improving operability as compared with endoscopy. Endoscopic assistance critically widens surgical exposure in blind spots without providing concomitant significant advantage in terms of surgical operability.**

INTRODUCTION

Great effort has been paid to the development of minimally invasive approaches to the intracranial space including endonasal-endoscopic techniques and keyhole craniotomies. However, minimally invasive approaches to intra-axial tumors are still limited.

Besides successful attempts to adapt endoscopic techniques to intra-axial surgery, it is becoming increasingly evident that microsurgical techniques still play a major role in the surgical armamentarium.[1]

Ventricular surgery represents a challenge even for modern neurosurgery due to approach-related risk of morbidity based on the potential damage of critical structures.[2,3]

Transcortical and transcallosal-interhemispheric routes have been applied for the resection of ventricular lesions.[4-7] Microsurgical approaches do usually require brain retraction, which has been demonstrated to increase the risk of damage of cortex and vascular structures.[1,8-10]

Endoscopic techniques have made possible a less invasive approach, with limited transection of brain tissue.[5,11-14] Ventricular endoscopy provided advantages in terms of reducing operating times and hospital stay.[5,15,16] However, operability is limited due

Key words
- Brain retraction
- Endoscopy
- Minimally invasive neurosurgery
- Tubular surgery
- Ventricular surgery

Abbreviations and Acronyms
aka: Also known as
CA: Central vision area
CE: Conizing effect
D: Depth of the surgical field
MAC: Maneuverability arc
MRI: Magnetic resonance imaging
OS: Operability score
PA: Peripheral vision area
SAA: Surgical angle of attack
VA: Vision area

From the Departments of [1]Neurosurgery and Gamma Knife Radiosurgery, San Raffaele Scientific Institute, Vita-Salute University, Milan, Italy; and [2]Neurological Surgery, The George Washington University, Washington, District of Columbia, USA

To whom correspondence should be addressed: Filippo Gagliardi, M.D., Ph.D. [E-mail: gagliardi.filippo@hsr.it]

Citation: World Neurosurg. (2019) 131:e255-e264.
https://doi.org/10.1016/j.wneu.2019.07.132

*Journal homepage: **www.journals.elsevier.com/world-neurosurgery***

*Available online: **www.sciencedirect.com***

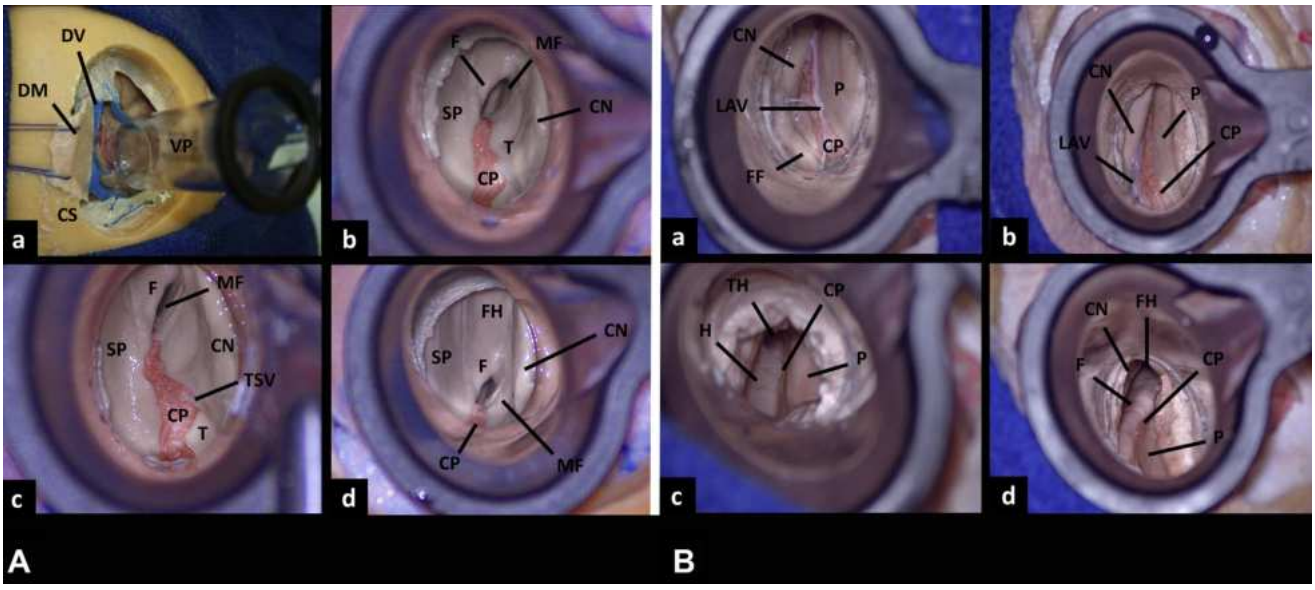

Figure 1. Microanatomic dissection. (**A**) Anterior (aka foraminal) approach. (*a*) Craniotomy and neuroport insertion. (*b*) Surgical view at Vycor neutral position. (*c*) Surgical view at Vycor −20-degree position (aka primary posterior position). (*d*) Surgical view at Vycor +20-degree position (aka primary anterior position). (**B**) Posterior (*aka* trigonal) approach. (*a* and *b*) Surgical view at Vycor neutral position. (*c*) Surgical view at Vycor −20-degree position (aka primary posterolateral position). (*d*) Surgical view at Vycor +20-degree position (aka primary anterior position). CN, caudate nucleus; CP, choroid plexus; CS, coronal suture; DM, dura mater; DV, draining vein; F, fornix; FF, fimbria fornix; FH, frontal horn; H, hippocampus; LAV, lateral atrial vein; MF, Monro foramen; P, pulvinar; SP, septum pellucidum; T, thalamus; TH, temporal horn; TSV, thalamostriate vein; VP, Vycor port.

to the restricted working channel and the impossibility for bimanual surgical manipulation.

Recently, portal systems for ventricular surgery have been considered as an option compared with endoscopic procedures and traditional transcortical approaches.[5]

The aim of this study was to describe and evaluate surgical exposure and operability of endoscopic-assisted tubular transcortical approaches to lateral ventricles. In particular, surgical freedom, area of exposure, and surgical field visualization have been taken into consideration. Technical limits and potentials are critically revised and discussed.

MATERIAL AND METHODS

Materials

Six cadaver specimens were used for anatomic dissections in the Ammerman Microsurgical Laboratory at George Washington University, Washington, D.C.

The heads were placed in surgical position and fixed in a Mayfield head-holder (Codman, Inc., Raynham, Massachusetts, USA).

Microsurgical dissections have been performed under a Zeiss OPMI 1-FC surgical microscope (Carl Zeiss Inc., Oberkochen, Germany), using Vycor ViewSite TC (Vycor Medical Inc., Boca Raton, Florida, USA) (21-mm/15-mm/7-cm device) as a tubular system and assisting the procedure with a rigid endoscope, 4 mm in diameter and 18 cm in length, with 0-, 30- and 45-degree lenses (Karl Storz Inc., Culver City, California, USA).

A high-speed drill was used for bone drilling (Midas Rex, Medtronic Inc., Fort Worth, Texas, USA).

Surgical Technique

Anterior Approach (Otherwise Known as foraminal). The head is fixed in a 3-point Mayfield head-holder in neutral position and slightly flexed (30° degrees). When possible, the nondominant side is preferred; nevertheless, the side of the approach has to be tailored according to the relative location of the lesion in the third or lateral ventricles. For this reason, during the dissections both sides have been used and evaluated.

A C-shaped skin incision is performed 2–3 cm lateral to the midline, crossing the coronal suture according to anatomic landmarks (Kocher point).

A 3 × 3 cm craniotomy is performed 1 cm anterior to the coronal suture at the intersection with the midpupillary line. The dura mater is opened, and the tubular retractor is inserted and smoothly advanced into the white matter to gain access to the frontal horn of the lateral ventricle.

The elliptical cross-section of the introducer and the conical shape of the tubular retractor facilitate progressive blunt-splitting of white fibers through the surgical path.

The tubular retractor is advanced 5–6 cm in depth until the lateral ventricle cavity is exposed (**Figure 1A**).

Posterior Approach (aka Trigonal). The head is fixed, slightly flexed (15–20 degrees), and rotated as much as possible to the contralateral side.

The entry point to the atrium and the posterior part of the temporal horn of the lateral ventricle corresponds to the Keen's point (aka the *posterior parietal point*).

Table 1. Measurements of Surgical Anatomy

	0 Degrees		−20 Degrees		+20 Degrees	
Depth of the surgical field	6.3 (±1.2) cm	N.s.	7.7 (±0.9) cm	N.s.	6.9 (±1.0) cm	N.s.
Depth of the surgical field	6.2 (±1.1) cm		8.6 (±0.2) cm		7.5 (±0.3) cm	
Central vision area	3.0 (±0.6) cm^2	N.s.	1.5 (±0.3) cm^2	N.s.	1.9 (±0.4) cm^2	N.s.
Central vision area	2.9 (±0.8) cm^2		1.7 (±0.6) cm^2		1.9 (±0.4) cm^2	
Peripheral vision area	4.0 (±0.4) cm^2	N.s.	11.8 (±5.4) cm^2	N.s.	8.1 (±2.2) cm^2	N.s.
Peripheral vision area	4.4 (±2.5) cm^2		12.9 (±3.5) cm^2		9.9 (±1.3) cm^2	
Maneuverability area	3.0 (±0.0) cm^2	N.s.	3.0 (±0.0) cm^2	n.s.	3.0 (±0.0) cm^2	n.s.
Maneuverability area	3.0 (±0.0) cm^2		3.0 (±0.0) cm^2		3.0 (±0.0) cm^2	
Maneuverability arc	34.8 (±1.5) degrees	N.s.	28.0 (±4.8) degrees	$P = 0.0224$	30.3 (±2.8) degrees	$P = 0.0342$
Maneuverability arc	35.7 (±3) degrees		21.8 (±1.6) degrees		26.7 (±1.0) degrees	
Surgical angle of attack	80.0 (±4.0) degrees	N.s.	68.8 (±6.0) degrees	N.s.	65.5 (±3.0) degrees	N.s.
Surgical angle of attack	81.0 (±3.7) degrees		69.7 (±3.3) degrees		61.3 (±4.5) degrees	

Colors: Measurements reported on the first raw for each variable correspond to those of the anterior approach; measurements reported on the second raw for each variable corresponds to those of the posterior approach.
N.s., not significant; 0 degrees, Vycor neutral position; −20 degrees, Vycor tilted 20 degrees posteriorly; +20 degrees, Vycor tilted 20 degrees anteriorly.

The horseshoe incision runs in the temporoparietal region with the concavity directed downward.

The center of the bone flap is placed 2.5–3 cm superior and 2.5–3 cm posterior to the top of the pinna.

The tubular retractor is advanced 4–5 cm perpendicular to the cerebral cortex toward the trigonal area (Figure 1B).

The application of neuronavigation for the assessment of the exact entry point and surgical trajectory is useful to minimize brain manipulation. The surgical trick we apply is to first introduce a navigation-guided ventricular catheter, which is used as a guide for the introducer toward the ventricular cavity. The introducer is preventively pierced on the bottom to allow catheter cannulation.

Once the ventricular cavity is reached, the introducer is removed and microsurgical instruments are advanced inside the working channel.

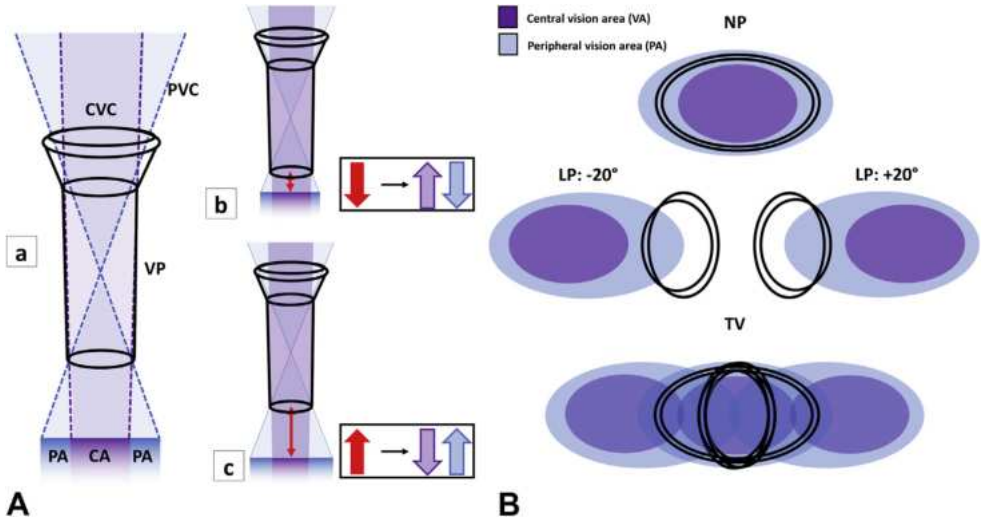

Figure 2. (**A**) Vision areas and geometric principle of portal view. (*a*) Nomenclature of vision areas. (*b*) Shorter is D (*red arrow*) larger is CA, and complementary smaller is PA. (*c*) Greater is D (*red arrow*), smaller is CA, and complementary larger is PA. (**B**) Schematic view of CA and VA in the 3 primary positions and resulting TV. CA, central vision area; CVC, central vision cone; LP, lateral position (±20 degrees corresponds to 20 degrees anterior or posterior tilting); NP, neutral position; PA, peripheral vision area; PVC, peripheral vision cone; TV, total vision area; VP, Vycor port.

Table 2. Operability Score

	0 Degrees	−20 Degrees	+20 Degrees
Depth of the surgical field	1	0	1
Depth of the surgical field	1	0	0
Maneuverability arc	1	0	1
Maneuverability arc	1	0	0
Surgical angle of attack	1	1	1
Surgical angle of attack	1	1	1
Operability score	3	1	3
Operability score	3	1	1

Colors: Measurements reported on the first raw of each variable correspond to those of the anterior approach; measurements reported on the second raw of each variable corresponds to those of the posterior approach.
0 degrees, Vycor neutral position; −20 degrees, Vycor tilted 20 degrees posteriorly; +20 degrees, Vycor tilted 20 degrees anteriorly.

The portal system is maintained in the desired position with a self-retaining retractor. The angle of incidence can be adjusted rotating the device around its own axis. Different angled endoscopic probes are introduced to improve direct visualization and panoramic view of target area.

Anthropometric Measurements and Operability Score

All measurements were obtained with graduated scales and calipers in triplicate to minimize data collection bias.

Mean and standard deviation of measurements were calculated for all specimens and reported in Table 1.

Anatomic and surgical areas, related to the different surgical approaches, were calculated using the software *ImageJ* 1.37 (National Institutes of Health, Bethesda, Maryland, USA).

The operability score (OS) was calculated as previously reported.[17]

Illustrative Case

The technique was adopted in a clinical setting. One illustrative case is reported to demonstrate technical feasibility.

RESULTS

Geometric Considerations

Vision area (VA) has been defined as the anatomic area explored though the Vycor in a fixed given position. It is composed by a *central vision area* (CA) and a *peripheral vision area* (PA) (Figure 2A). CA is defined as the area, visualized by pointing the microscope directly in the center of the portal corridor. Alternatively, PA is

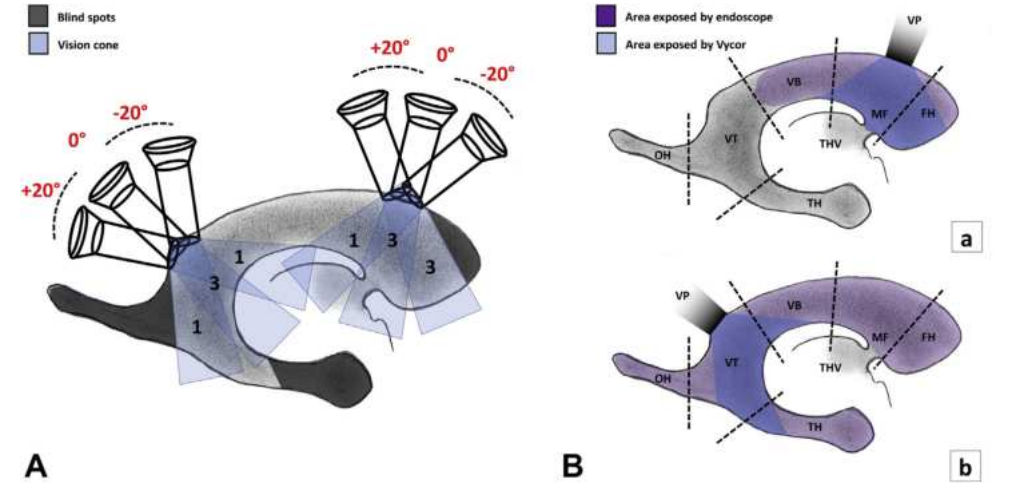

Figure 3. (**A**) Schematic view of different vision cones according to Vycor's primary positions in both approaches and blind spots. Numbers correspond to the values of the operability score. (**B**) Schematic view of exposed areas. It has to be underlined that port-tilting is schematized; in the real scenario, the port swivels much closer to the cortical entry site. FH, frontal horn; MF, Monro foramen; OH, occipital horn; TH, temporal horn; THV, third ventricle; VB, ventricular body; VP, Vycor port; VT, ventricular trigone.

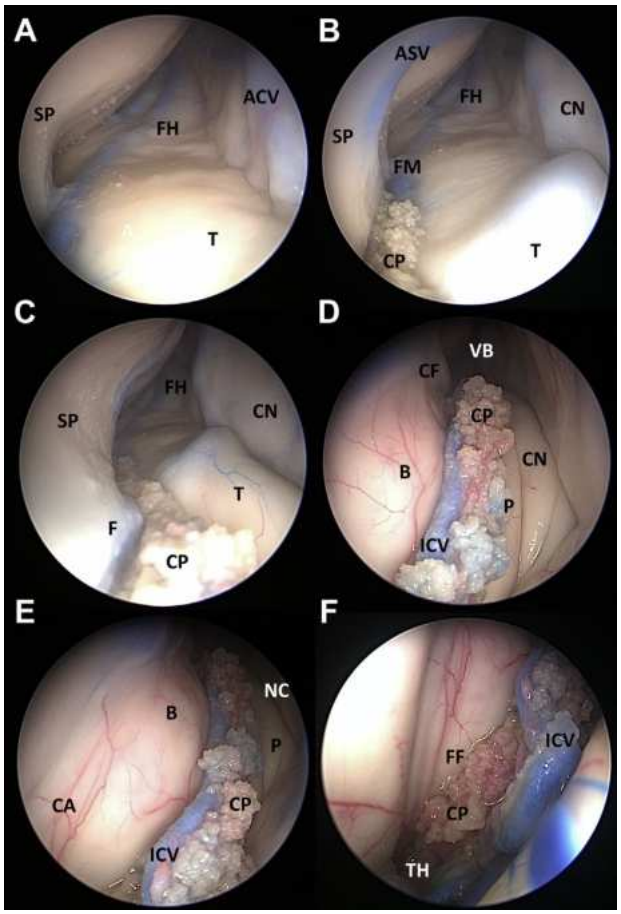

Figure 4. Posterior view of the right lateral ventricle. An endoscopic probe has been inserted through a Vycor portal system in the atrium of the ventricle. (**A**) Frontal horn of the lateral ventricle. (**B**) Enlarged view of the foramen of Monro, which delimitates the frontal horn from the body of the lateral ventricle. (**C**) Body of the lateral ventricle. (**D**) Upper and (**E**) lower part of the atrium of the lateral ventricle. Anteriorly the atrium communicates with the body of the ventricle above the thalamus, and with the temporal horn below the thalamus. (**F**) Posterior opening of the temporal horn of the lateral ventricle. ACV, anterior caudate vein; ASV, anterior septal vein; B, bulb of the corpus callosum; CA, calcar avis; CF, crus fornix; CN, caudate nucleus; CP, choroid plexus; F, fornix; FF, fimbria fornix; FH, frontal horn; FM, foramen of Monro; ICV, inferior choroidal vein; P, pulvinar; TH, temporal horn; T, thalamus; SP, septum pellucidum; VB, ventricular body.

defined as the area surrounding the CA and corresponding to the adjunctive area of vision, obtained by tilting the microscope in the extreme lateral positions (see Figure 2A). Both CA and PA are correlated to the *depth of the surgical field* (D); according to the principle of the *conizing effect* (CE), as already described,[17] greater is D, smaller is CA, and complementary larger is PA (see Figure 2A).

As experienced in the real scenario, by tilting the Vycor side to side by an angle of ±20 degrees, total VA (total vision) consists of the geometric sum of the single VAs, as calculated in the 3 primary positions: neutral (aka 0 degrees), +20 degrees, and −20 degrees (see Figure 2B).

Port tilting of ±20 degrees almost duplicates the visual area as obtained in the neutral position alone (×1.66) with a significant increase of >2 times of CA (×2.66) (see Figure 2B).

Mean D, CA, and PA values calculated in the primary positions are reported in Table 1.

According to OS, the *maneuverability area* is considered as the cross-section area of the surgical corridor at its narrowest point; in the present study, it corresponds to the narrowest cross-section of the port. Because we always applied the Vycor ViewSite TC (21 mm/15 mm/7 cm device), the maneuverability area must be considered as a constant and corresponds to 3 cm^2, making CE directly dependent to D.

The *maneuverability arc* (MAC) is defined as the degree of freedom in manipulating surgical instruments. Being influenced by CE, it is inversely proportional to D. Mean MAC values are reported in Table 1.

The *surgical angle of attack* (SAA) is defined as the angle of incidence of the surgical corridor in the surgical field. Particularly, in the present study, SAA corresponds to the angle of incidence of the major axis of the neuroport toward the surgical field. Mean SAA values are reported in Table 1.

According to OS, a score of either 0 or 1 was assigned to each quantitative variable. For D the assigned score was 0 if D was >7 cm and was 1 if it was <7 cm. For MAC, to a calculated value of >30 degrees, the assigned score was 1 and to those calculated of <30 degrees, the assigned score was 0. To an SAA wider than 60 degrees, the assigned score was 1, and to those <60 degrees in width the assigned score was 0.

The sum of the 3 scores assigned to the single variables in each of the primary positions, in both anterior and posterior approaches, corresponds to the overall OS value in that position. The OS ranged from a minimum of 0 to a maximum of 3 (Table 2).

Anatomic Considerations

By performing the anterior approach (aka the foraminal approach), Vycor neutral position corresponds to the Vycor major axis targeting the Monro foramen and periforaminal area; +20 degrees (aka primary anterior position) corresponds to the Vycor position tilted 20 degrees anteriorly, targeting the ventricular frontal horn; alternatively, −20 degrees (aka primary posterior position) corresponds to the Vycor position tilted 20 degrees posteriorly targeting the ventricular atrium and body (see Figure 1A and 3A).

By performing the posterior approach (aka trigonal approach), Vycor neutral position corresponds to the Vycor major axis targeting the ventricular trigone; +20 degrees (aka primary anterior position) corresponds to the Vycor position tilted 20 degrees anteriorly, targeting the ventricular body and atrium; alternatively, −20 degrees (aka primary posterolateral position) corresponds to the Vycor position tilted 20 degrees posteriorly and laterally targeting the ventricular temporal horn (see Figures 1B and 3A).

Vision provided by portal corridors is limited by 3 major blind spots. In the foraminal approach the main one is located in the most anterior part of the roof of the frontal horn; in the trigonal approach, the first one is the occipital horn and the second one the most anterior aspect of the temporal horn (see Figure 3B).

Application of endoscopy significantly increases surgical exposure, however, without providing a concomitant significant

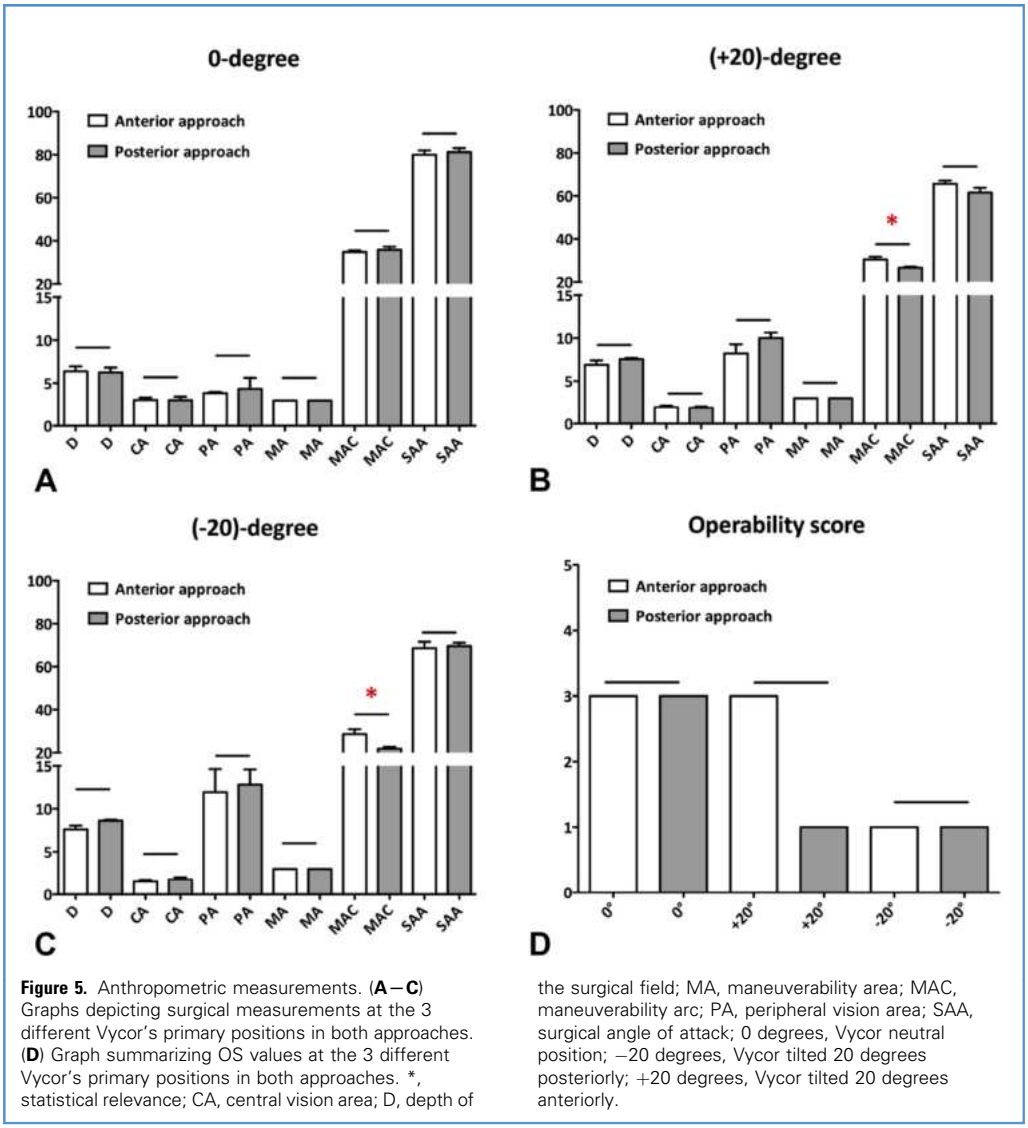

Figure 5. Anthropometric measurements. (**A**–**C**) Graphs depicting surgical measurements at the 3 different Vycor's primary positions in both approaches. (**D**) Graph summarizing OS values at the 3 different Vycor's primary positions in both approaches. *, statistical relevance; CA, central vision area; D, depth of the surgical field; MA, maneuverability area; MAC, maneuverability arc; PA, peripheral vision area; SAA, surgical angle of attack; 0 degrees, Vycor neutral position; −20 degrees, Vycor tilted 20 degrees posteriorly; +20 degrees, Vycor tilted 20 degrees anteriorly.

increase of surgical operability. In the foraminal approach, the endoscope enhances one's view in the blind spot represented by the frontal horn and widens the surgical view in the most posterior aspect of the ventricular body. In the trigonal approach, due to the favorable SAA, the endoscope enables the surgeon to visualize the entire ventricular cavity and, by applying angulated lenses, even the blind spots corresponding to the occipital and temporal horns (see Figures 3B and 4).

Comparative Analysis

Comparative analysis of single variables confirms in both approaches overlapping values, except for a significant difference in the MAC, as recorded at the primary anterior and posterior positions.

By comparing OS in the 3 primary positions, the maximal scores (OS 3) were recorded in Vycor neutral positions while the minimal scores (OS 1) were recorded in the primary posterior positions in both approaches. The only significant difference in OS was recorded in the primary anterior position between the anterior (OS 3) and posterior approach (OS 1) due to the significant differences in terms of D and MAC (Figure 5).

Illustrative Case

We report the case of a 49-year-old man affected by an anaplastic astrocytoma (2016 World Health Organization grade III) originating from the pulvinar and lateral geniculate body of the right thalamus (Figure 6).

Three-point fixation was achieved with the patient in lateral position by tilting the head slightly to the left. Registration with frameless stereotactic image-guided neuronavigation software (Brainlab Cranial 3.0 Navigation, Munich, Germany) was obtained and used to plan the keyhole parietal craniotomy, as well as the trajectory for the insertion of Vycor ViewSite Brain Access System (21 mm × 15 mm × 7cm).

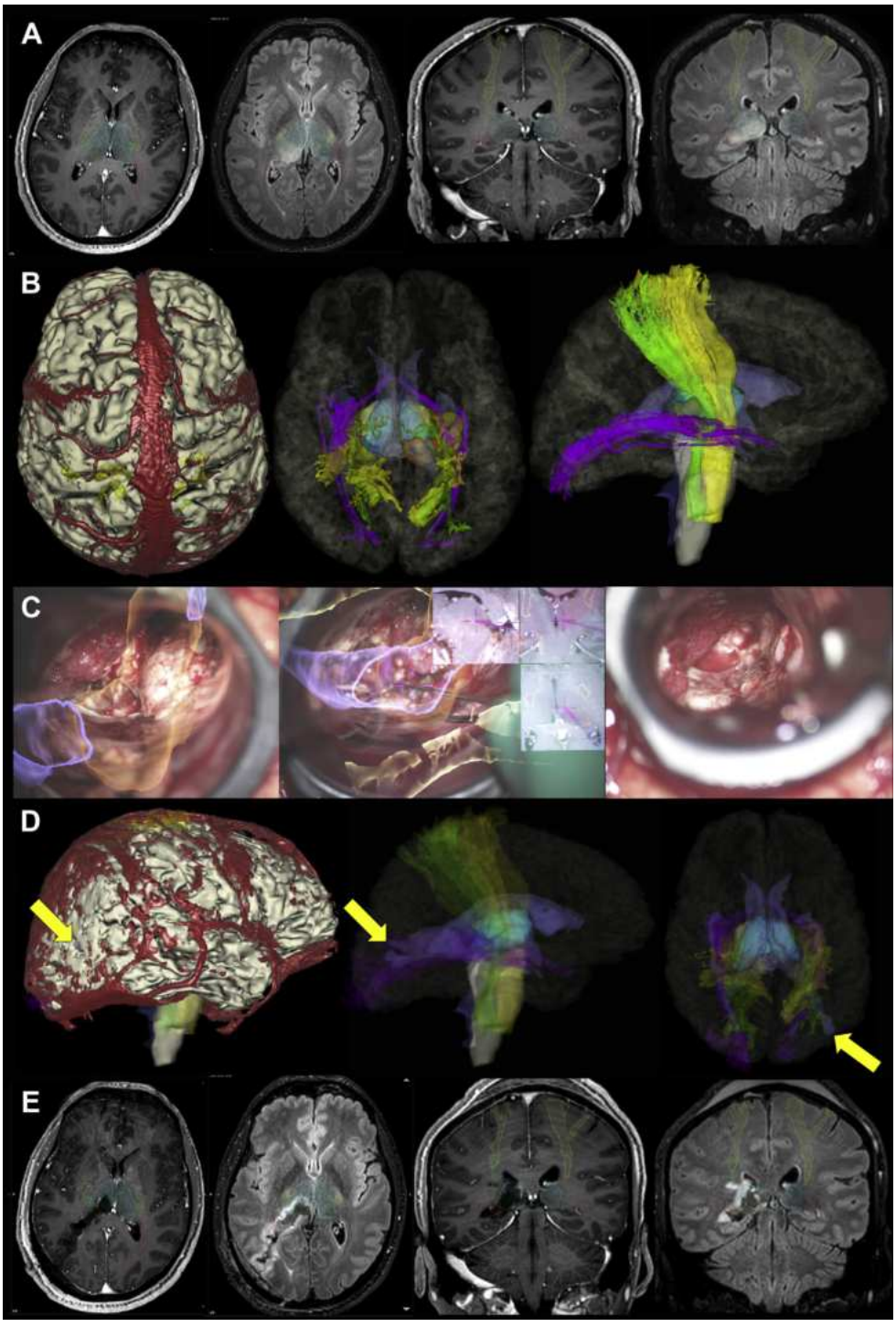

The tubular retractor was carefully advanced into the brain parenchyma toward the ependymal walls of the right lateral ventricle atrium. The boundaries of the thalamic tumor were identified with the aid of the neuronavigation system integrated with preoperative magnetic resonance imaging (MRI) tractography data, such that major eloquent white fiber tracks would be avoided.

As debulking proceeded with standard microsurgical techniques through the portal working channel, the trajectory of the

retractor was adjusted to visualize the margins of the tumor and surrounding structures. The mass was removed in a gross total fashion.

After obtaining hemostasis in the surgical bed, the retractor was loosened and slowly withdrawn, cauterizing bleeding sources identified through the transparent wall of the retractor along the surgical pathway in the white matter.

A 24-hour postoperative MRI and diffusion tensor imaging (DTI) demonstrated mild alteration of signal intensity in T2/fluid-attenuated inversion recovery sequences corresponding to limited white matter traumatic injury due to tubular retractor insertion. Part of the superior aspect of the optic radiations, covering the roof of the most posterior part of atrium and occipital horn, was sacrificed during the intervention in order to reach the lesion with the optimal approach and angle.

The patient hence suffered from inferior right homonymous quadrantanopia postoperatively. The recovery was good, and he was discharged 5 days after surgery.

DISCUSSION

Resection of intraventricular lesions remains a challenge even for modern neurosurgery, due to the risk of damage to critical anatomic structures.[2,3] Historically, transcortical and transcallosal interhemispheric approaches have been applied. Significant complications have been associated with transcortical routes, while cognitive impairment due to Papez circuit structures damage has been advocated as the main drawback of transcallosal approaches.[18]

In 1980, Greenberg introduced the application of self-locking retractors in transcortical routes to deep-seated lesions.[19] Recent experience has shown that the main drawback of this technique, retractor-associated injury, is due to direct pressure and local ischemia.[1,8-10,20,21]

In recent decades, the great advancements made in endoscopic techniques led to a less invasive transcortical approach with limited transection of healthy brain tissue, as well as to a reduction in operating times and hospital stay compared with traditional microsurgical routes.[11-16] Endoscopic techniques, however, do not allow for bimanual microsurgical manipulation, significantly reducing surgical maneuverability.[5]

The first experiences using tubular retractor systems affixed to frame-based stereotaxis systems for the resection of intraaxial deep-seated lesions, such as thalamic tumors, were described in the late 1980s.[22-25] In 2005, Harris et al[26] first applied a thoracic port for use as a stereotactic transcortical corridor for endoscopically guided microsurgical resection of ventricular tumors, reporting minimized brain retraction and satisfactory visualization.

Notably, transcortical intrusion of narrow retractors and endoscopes has been demonstrated to minimize regional corticectomy and brain disruption. Cylindrical systems cause minimal focal tissue damage on the basis of the fact that retraction pressure is homogenously distributed over a wide area as compared with traditional blades.[27] Port-related minimal tissue disruption is supported by minimal fluid-attenuated inversion recovery/T2 change and diffusion restriction noted along surgical trajectories on early postoperative MR images.[1]

In 1989 this concept was validated by Kelly et al,[22-24] observing how tubular retractors did equally distribute retaining pressure along their smooth surface, minimizing brain injury as compared with traditional blades, which stretch and occlude vascular feeders, causing ischemic injury. Regional cerebral blood flow is affected and can reach critical ischemic levels when brain retraction pressures exceed 20 mm Hg.[24,28,29] Tubular retractors by largely distributing forces on surrounding tissues provide a brain retraction pressure of $<$10 mm Hg.[30]

As compared with a traditional working channel of purely endoscopic procedures (6–8 mm), those provided by minitubular retractors are wider and not different in terms of mechanical injury on brain parenchyma from that provided by endoscopes.[5]

For the port's insertion, both transulcal and transcortical approaches have been described and applied according to the location of the lesion. The transulcal approach is slightly more challenging, requiring a fine arachnoidal dissection with sulcal vessel manipulation. We recommend its application for relatively superficial lesions; in those cases, the use of a transulcal route might significantly reduce parenchymal manipulation. For deep-seated lesions, the transcortical route is easier and relatively safer.

In the present experience, transcortical insertion was used through 2 main approaches: anterior (aka foraminal) and posterior (aka trigonal). Through the anterior approach, a neuroport provides maximal operability (OS 3) in the periforaminal area and posterior aspect of the frontal horn, while through the posterior approach maximal operability is achieved in the paratrigonal area. Minimal scores (OS 1) were recorded in primary posterior positions in both approaches. MAC and D were the most significant variables affecting OS.

Endoscopic assistance does not improve operability but provides adjunctive exposure in blind spots as the roof of the frontal horn and the most anterior aspect of the temporal and occipital horn.

Literature data report that a diameter of 17 mm, as that of the port used in the present study, allows stereoscopic vision with

Figure 6. Illustrative case. (**A**) Axial and coronal slices of preoperative T1 contrast-enhanced and fluid-attenuated inversion recovery (FLAIR) magnetic resonance sequences; the contours of the tumor (orange), thalamus (light blue), corticospinal tracts (yellow), somatosensory (green), and visual (purple) pathways are plotted. (**B**) 3-Dimensional reconstruction of the cortical surface and vessels (left) and of the deep structures and eloquent fibers (right); ventricles (blue) are also represented. **(C)** Intraoperative view during the resection using the portal system Vycor ViewSite TC and augmented reality (Brainlab Microscope and Cranial 3.0 Navigation). The tumor volume (orange) and the right lateral ventricle (blue) were injected in the microscopic scene (left). The final check with neuronavigation was at the end of the resection (center). The surgical cavity before the final hemostasis is also shown (right). **(D)** 3-D reconstruction of the cortical surface and vessels (left) and of the deeper structures and fibers (right), as well as the small site of corticectomy *(arrows)*. **(E)** Axial and coronal slices of T1 contrast-enhanced and fluid-attenuated inversion recovery magnetic resonance sequences acquired 24 hours postoperatively.

surgical microscopes, permitting 2-handed surgery with standard microsurgical instruments. Use of transphenoidal instruments increases surgical maneuverability.[1]

Further possibility to intraoperatively adjust surgical corridor direction, by slightly tilting the port, significantly increases surgical exposure beyond the cross-section area of the tube. Limited portal tilting does not generate critical stress on brain parenchyma as demonstrated by a biomedical engineering model.[31] Starting from our surgical experience, we tilted the Vycor side to side by an angle of ±20 degrees in relation to its neutral position. In our daily clinical practice by tilting the port, after its insertion, we did not find any significant increase in fluid-attenuated inversion recovery alterations on postoperative MRI, as compared with its maintenance in a given position for the entire procedure; moreover, any adjunctive perioperative morbidity has been recorded. TV ultimately consists of the geometric sum of single VA, as calculated in the 3 primary positions: neutral (aka 0 degrees), +20 degrees, and −20 degrees. We found that port tilting almost duplicates the visual area as obtained in the neutral position alone (×1.66).

The transparent wall of the port provides good visualization of surrounding tissue, and the elliptical shape further widens surgical maneuverability. Moreover, the smooth surface of the introducer allows gradual retraction of underlying white fibers and atraumatic splitting might preserve their anatomic and functional integrity as opposed to fiber transection occurring with traditional blades.[1,5]

Due to the enlarged maneuverability area and maneuverability arch of surgical instruments, portal surgery is feasible even in case of patients without hydrocephalus, who may be not good candidates for endoscopic procedures.[5]

Development of endoscopic techniques, minimizing cortical injury, has sensibly reduced iatrogenic epileptic sequelae, compared with traditional transcortical routes.[5,32] It is reasonable to expect comparable results from portal surgery because of the previously mentioned evidences, yet a randomized comparative evaluation to postulate that would be necessary, which is far from the aim of this study.

CONCLUSION

Ventricular tubular systems provide adequate visualization, with minimal brain retraction, improving operability as compared with traditional endoscopy. Minimal port tilting (±20 degrees) provides a 2× increase of the surgical view. Endoscopic assistance further widens surgical exposure in blind spots without providing concomitant significant advantage in terms of surgical operability. Portal surgery with endoscopic assistance might be considered an effective option in the armamentarium of modern neurosurgery for the resection of large lesions in the lateral ventricles.

ACKNOWLEDGMENTS

The authors want to acknowledge Brainlab for providing the opportunity to use the Brainlab Microscope and Cranial 3.0 Navigation and, in particular, Gaia Tonani and Domenico Barillà for their support.

REFERENCES

1. Raza SM, Recinos PF, Avendano J, Adams H, Jallo GI, Quinones-Hinojosa A. Minimally invasive trans-portal resection of deep intracranial lesions. *Minim Invasive Neurosurg*. 2011;54:5-11.
2. Mortini P, Gagliardi F, Bailo M, et al. Resection of tumors of the third ventricle involving the hypothalamus: effects on body mass index using a dedicated surgical approach. *Endocrine*. 2017;57:138-147.
3. Mortini P, Gagliardi F, Boari N, Roberti F, Caputy AJ. The combined interhemispheric subcommissural translaminaterminalis approach for large craniopharyngiomas. *World Neurosurg*. 2013;80:160-166.
4. Abernathey CD, Davis DH, Kelly PJ. Treatment of colloid cysts of the third ventricle by stereotaxic microsurgical laser craniotomy. *J Neurosurg*. 1989;70:525-529.
5. Cohen-Gadol AA. Minitubular transcortical microsurgical approach for gross total resection of third ventricular colloid cysts: technique and assessment. *World Neurosurg*. 2013;79:207-210.
6. Decq P, Le Guerinel C, Brugieres P, et al. Endoscopic management of colloid cysts. *Neurosurgery*. 1998;42:1288-1294.
7. Morita A, Kelly PJ. Resection of intraventricular tumors via a computer-assisted volumetric stereotactic approach. *Neurosurgery*. 1993;32:920-926.
8. Rosenorn J, Diemer N. The risk of cerebral damage during graded brain retractor pressure in the rat. *J Neurosurg*. 1985;63:608-611.
9. Rosenorn J, Diemer NH. Reduction of regional cerebral blood flow during brain retraction pressure in the rat. *J Neurosurg*. 1982;56:826-829.
10. Zhong J, Dujovny M, Perlin AR, Perez-Arjona E, Park HK, Diaz FG. Brain retraction injury. *Neurol Res*. 2003;25:831-838.
11. Abdou MS, Cohen AR. Endoscopic treatment of colloid cysts of the third ventricle. Technical note and review of the literature. *J Neurosurg*. 1998;89:1062-1068.
12. Hellwig D, Bauer BL, Schulte M, Gatscher S, Riegel T, Bertalanffy H. Neuroendoscopic treatment for colloid cysts of the third ventricle: the experience of a decade. *Neurosurgery*. 2008;62(suppl 3):1101-1109.
13. Horn EM, Feiz-Erfan I, Bristol RE, et al. Treatment options for third ventricular colloid cysts: comparison of open microsurgical versus endoscopic resection. *Neurosurgery*. 2008;62(suppl 3):1076-1083.
14. Rodziewicz GS, Smith MV, Hodge CJ Jr. Endoscopic colloid cyst surgery. *Neurosurgery*. 2000;46:655-660.
15. Kehler U, Brunori A, Gliemroth J, et al. Twenty colloid cysts—comparison of endoscopic and microsurgical management. *Minim Invasive Neurosurg*. 2001;44:121-127.
16. Lewis AI, Crone KR, Taha J, van Loveren HR, Yeh HS, Tew JM Jr. Surgical resection of third ventricle colloid cysts. Preliminary results comparing transcallosal microsurgery with endoscopy. *J Neurosurg*. 1994;81:174-178.
17. Gagliardi F, Boari N, Roberti F, Caputy AJ, Mortini P. Operability score: an innovative tool for quantitative assessment of operability in comparative studies on surgical anatomy. *J Craniomaxillofac Surg*. 2014;42:1000-1004.
18. Milligan BD, Meyer FB. Morbidity of transcallosal and transcortical approaches to lesions in and around the lateral and third ventricles: a single-institution experience. *Neurosurgery*. 2010;67:1483-1496.
19. Greenberg IM. Self-retaining retractor and handrest system for neurosurgery. *Neurosurgery*. 1981;8:205-208.
20. Albin MS, Bunegin L. The insidiousness of brain retractor pressure: another "Smoking gun"? *Anesth Analg*. 2003;96:306.
21. Donaghy RM, Numoto M, Wallman LJ, Flanagan ME. Pressure measurement beneath retractors for protection of delicate tissues. *Am J Surg*. 1972;123:429-431.
22. Kelly PJ. Future perspectives in stereotactic neurosurgery: stereotactic microsurgical removal of deep brain tumors. *J Neurosurg Sci*. 1989;33:149-154.

23. Kelly PJ, Goerss SJ, Kall BA. The stereotaxic retractor in computer-assisted stereotaxic microsurgery. Technical note. *J Neurosurg*. 1988;69:301-306.

24. Kelly PJ, Kall BA, Goerss SJ. Computer-interactive stereotactic resection of deep-seated and centrally located intraaxial brain lesions. *Appl Neurophysiol*. 1987;50:107-113.

25. Moshel YA, Link MJ, Kelly PJ. Stereotactic volumetric resection of thalamic pilocytic astrocytomas. *Neurosurgery*. 2007;61:66-75.

26. Harris AE, Hadjipanayis CG, Lunsford LD, Lunsford AK, Kassam AB. Microsurgical removal of intraventricular lesions using endoscopic visualization and stereotactic guidance. *Neurosurgery*. 2008;62(suppl 2):622-629.

27. Barlas O, Karadereler S. Stereotactically guided microsurgical removal of colloid cysts. *Acta Neurochir (Wien)*. 2004;146:1199-1204.

28. Andrews RJ, Bringas JR. A review of brain retraction and recommendations for minimizing intraoperative brain injury. *Neurosurgery*. 1993;33:1052-1063.

29. Recinos PF, Raza SM, Jallo GI, Recinos VR. Use of a minimally invasive tubular retraction system for deep-seated tumors in pediatric patients. *J Neurosurg Pediatr*. 2011;7:516-521.

30. Ogura K, Tachibana E, Aoshima C, Sumitomo M. New microsurgical technique for intraparenchymal lesions of the brain: transcylinder approach. *Acta Neurochir (Wien)*. 2006;148:779-785.

31. Francois PM, Sandoz B, Decq P, Laporte S. Quantification of the stress generated by the endoscopic movement in the brain parenchyma during intra ventricular surgical procedure. *Comput Methods Biomech Biomed Engin*. 2017;20(suppl 1):79-80.

32. Solaroglu I, Beskonakli E, Kaptanoglu E, Okutan O, Ak F, Taskin Y. Transcortical-transventricular approach in colloid cysts of the third ventricle: surgical experience with 26 cases. *Neurosurg Rev*. 2004;27:89-92.

Conflict of interest statement: The authors have nothing to disclose. This research did not receive any specific grant from funding agencies in the public, commercial, or not-for-profit sectors.

Received 18 April 2019; accepted 16 July 2019

Citation: World Neurosurg. (2019) 131:e255-e264.
https://doi.org/10.1016/j.wneu.2019.07.132

Journal homepage: ***www.journals.elsevier.com/world-neurosurgery***

Available online: ***www.sciencedirect.com***

1878-8750/$ - see front matter